Charge Density Studies of Weak Interactions in Dipicrylamine†

Krzysztof Woźniak*

Chemistry Department, Warsaw University, 02 093 Warszawa, ul. Pasteura 1, Poland

Paul R. Mallinson

Chemistry Department, University of Glasgow, Glasgow G12 8QQ, U.K.

Chick C. Wilson

ISIS Fascility, Rutherford Appleton Laboratory, Chilton, Didcot, Oxon OX11 0QX, U.K.

Eric Hovestreydt

Brucker AXS GMBH., Östl., Rheinbrückenstr. 50, D-76187 Karlsruhe, Germany

Eugeniusz Grech

Institute of Chemistry and Enviromental Protection, Technical University of Szczecin, Piastów 42, 71 065 Szczecin, Poland

Received: December 31, 2001; In Final Form: April 8, 2002

A low-temperature high-resolution X-ray and neutron diffraction study of charge distribution in the superacid dipicrylamine (DPA) has been carried out. This structure exhibits interesting weak interactions including bifurcated N−H···O and C−H···O H-bonds which consolidate it. The corresponding interaction lines appear to be modified in the vicinity of the critical points of the covalent bonds of the hydrogen atoms. The presence of six nitro groups generates some short N···O contacts. On the basis of the experimental interaction paths, an attractive interaction is found, in agreement with the prediction of such an effect from earlier model ab initio calculations performed for simple dimers. For these weak interactions, a linear relationship is found between the charge density at the interaction critical points and the N−O distance.

Introduction

The understanding of the packing in crystalline lattices and the subsequent generation of "engineered" interactions between pre-selected constituent blocks in the resulting assemblies form the basis of modern-day crystal engineering. The weaker types of interaction, such as C−H···C, C−H···O, and C−H···π, not only generate such structures but they play a crucial role in many chemical and biological systems, since they can be switched on and off with energies which correspond to small temperature fluctuations. Crystal packing, molecular conformation, molecular recognition processes, stabilization of inclusion complexes, stability, and, possibly, activity of biological molecules are all influenced by or depend on the directionality of hydrogen bonds; the numerous possibilities for the formation of these weaker types (compared with the well-known strong bonds O−H···O, N−H···O, etc.) make them of paramount importance. The topicality of this area of chemistry is exemplified by the following articles.[1−3]

An important class of weak, directional interactions comprises C−H...O hydrogen bonds, which have typical bond energies around 5 kJ/mol.[4] Most work to date has focused on their characterization by the "crystal correlation" technique in which geometrical features are analyzed statistically on the basis of a large amount of published structural data available in the Cambridge Structural Database.[5] Recently Koch and Popelier[6] have demonstrated an alternative approach: the theory of "atoms in molecules" (AIM)[7] can be used to characterize weak interactions on the basis of theoretical charge density (CD) distributions in the donor and acceptor molecules and in intermolecular regions. Such an informative analysis of both the theoretical and experimental charge density is based upon the topological properties of the density $\rho(\mathbf{r})$. Any bonded pair of atoms has a bond path, i.e., a line of the highest electron density linking them. The point on this line where the gradient of rho, $\nabla\rho(\mathbf{r})$, is equal to zero, is termed the bond critical point (CP), and the properties of the density at this point give quantitative information on that bond's characteristics. A bond path between a pair of nonchemically bonded atoms is called an interaction line. The Laplacian of the density ($\nabla^2\rho(\mathbf{r})$) contains a large amount of chemical information. Since this is the second derivative of the electron density, it indicates where the density is locally concentrated ($\nabla^2\rho(\mathbf{r}) < 0$) and depleted ($\nabla^2\rho(\mathbf{r}) > 0$) and, hence, graphically shows features such as bonds and lone pairs, which are not observable in $\rho(\mathbf{r})$ itself. Espinosa, Molins and Lecomte[8] have analyzed H-bond strengths in terms of the experimental kinetic and potential energy densities at the critical points (CP), using published, experimentally observed electron density data. An interesting AIM analysis of ab initio (DFT and MP2) studies of intermolecular

† Dedicated to Prof. T. M. Krygowski on his 65th birthday.

* To whom correspondence should be addressed. Chemistry Department, Warsaw University, 02 093 Warszawa, ul. Pasteura 1, Poland. Phone/fax: +48 22 8222892. E-mail: kwozniak@chem.uw.edu.pl.

10.1021/jp014733x CCC: $22.00
Published on Web 06/25/2002

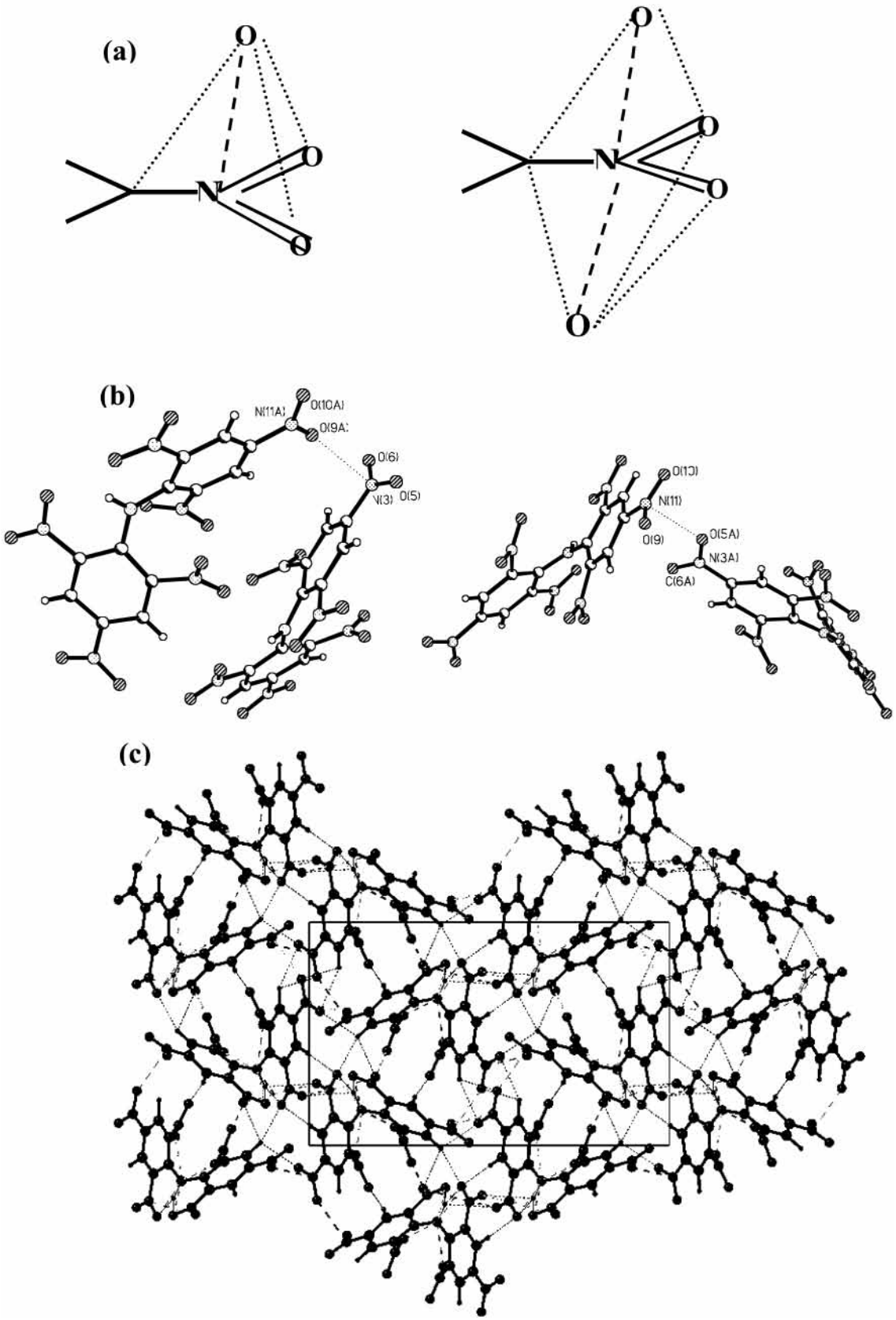

Figure 1. (a) Structural patterns formed by terminal oxygen atoms and a nitro group, (b) selected examples of attractive N···O interactions in the DPA crystal lattice: N(3)···O(9) [$1 - X$, $-0.5 + Y$, $-0.5 - Z$] and N(11)···O(5) [$1.5 - X$, $1 - Y$, $-0.5 + Z$]), (c) arrangement of DPA molecules in 3D crystal lattice, showing coexistence of weak C−H···O H-bonds (dotted lines) and attractive N···O interactions (dashed lines).

C−H···O hydrogen bonds has recently been published by Wang and Balbuena.[9]

Some of the weakest hydrogen bonds, formed between C−H groups and olefinic or aromatic π-electron systems, have energies up to a few kJ/mol.[10,11] Within the past few years weaker and weaker interactions have been proved to play an important role in the formation of 3D structures of organic and inorganic solids. C−H···O, C−H···N, and C−H···C hydrogen

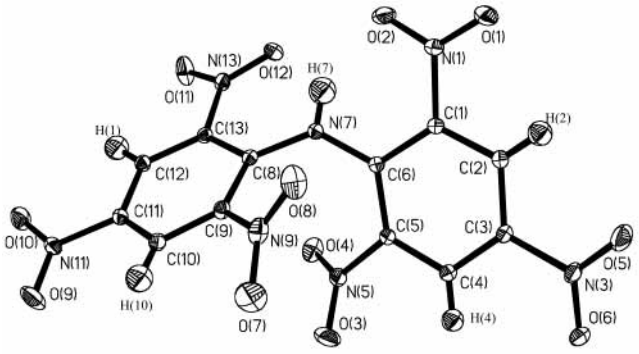

Figure 2. Labeling scheme and thermal vibration ellipsoids at 50% probability level for DPA.

bonds and X···X (where X is Cl, Br, or N) contacts are good examples of such weak interactions. Also, a possibility of attractive interactions between −CO and −CN groups has been examined,[12] although the conclusions of this paper were negative.

The study of *N*,*N*-dipicrylamine and related compounds[13−15] demonstrated a new class of weak intermolecular N···O interactions. Many close approaches—shorter than the sum of the van der Waals radii—for the nitrogen in RNO_2 groups and the terminal oxygen atoms in neighboring molecules have been found. The oxygen atoms from the neighboring molecules tend to form with the $-NO_2$ structural fragment regular patterns such as pyramids and bipyramids (Figure 1a,b) which is well illustrated in the DPA crystal lattice shown in Figure 1c.

This suggests that, as in the case of hydrogen bonds, the N···O interactions should be vectorial in nature and sensitive to stereochemistry. According to ab initio calculations,[14] the energy of such interactions is comparable in strength with weak hydrogen bonds. Dimer binding energies of 10−13 kJ/mol were obtained at the optimal N···O distance of ca. 2.85 Å at the MP2/6-31++G** level, which is close to the energies characteristic for weak H-bonds, such as C−H···O and C−H···N. Atoms-in-molecules calculated charge distribution suggests that these interactions are dominated by dispersive forces. Just as in the case of the weaker types of the H-bonds, the N···O interactions can be statistically analyzed in terms of the average values of structural parameters.[15]

Since according to the ab initio calculations, the N···O interactions appear to be sufficiently strong to compete with other types of weak interactions in the ordering of molecular and biological systems, we aim to study their nature by neutron

TABLE 1: Experimental X-ray and Neutron Data for Dipicrylamine (DPA)

formula	$C_{12}H_5N_7O_{12}$
formula weight	439.19
temperature	100(2) K
space group	$P2_12_12_1$ (orthorhombic)
unit cell dimensions /å	$a = 7.3586(1)$
	$b = 11.6401(2)$
	$c = 18.7345(4)$
volume/Å^3	1604.70(5)
Z	4
D_c/Mg m^{-3}	1.818
F(000)	816
radiation	Mo Kα; $\lambda = 0.71073$ Å
diffractometer	SMART CCD
max{[sin(θ)/λ], 2θ}	1.196 Å^{-1}, 116.62^o
crystal dimensions/mm	0.25 × 0.30 × 0.25
absorption coefficient/cm^{-1}	1.7
Index ranges: min. max	−12,14; −20,27; −34,44;
no. of reflections measured	60996
no. of symmetry-independent reflections	20370
no. of reflections with $F_o > 4\sigma(F_o)$	16677
agreement factor R_{int}	0.043
refinement method	full-matrix least-squares on F
N_{obs}/N_{var}	21
goodness-of-fit on F	0.960
final R indices	$R = 0.030$, $R_w = 0.034$
weighting scheme	$w = 1/\sigma^2(F) = 4F^2/\sigma^2(F^2)$
	where $\sigma^2(F^2) = \sigma^2_{counting}(F^2) + P^2F^4$
positional and thermal parameters for H-atoms taken from neutron diffraction	
neutron data	
collection method and site	time-of-flight Laue diffraction, instrument SXD, ISIS pulsed neutron source (RAL, U.K.)
neutron wavelength	0.5−5 Å
temperature	100 K
crystal size/mm	4 × 3 × 3
θ range for neutron data collection	1.4−46°
$(\sin\theta/\lambda)_{max}$ for $\lambda = 0.7107$/Å^{-1}	1.012
index ranges: min, max	−16,16; −29,29; −63,63;
refinement method for neutron data	full-matrix least squares on F^2
agreement factor R_{int}	0.056
no. of unique reflections with $F_o > 4\sigma(F_o)$	3980
restraints/parameters	0/325
goodness-of-fit on F^2	1.067
final R indices	$R = 0.0538$, $R_w = 0.1150$
weighting scheme	$1/[\sigma^2(F_o^2) + (0.0697P)^2 + 11.73P]$
	where $P = (\max(F_o^2,0) + 2F_c^2)/3$

TABLE 2: Inter- and Intramolecular Interactions in DPA

interaction[a]	symmetry code	ρ [eÅ^{-3}]	$\nabla^2\rho$ [eÅ^{-5}]	internuclear distance [Å]	angle at H-atom
N···O					
N(1)···O(3)	[1 − *X*, −0.5 + *Y*, 0.5 − *Z*]	0.02	0.4	3.110(1)	
N(1)···O(11)	[1 + *X*, *Y*, *Z*]	0.01	0.2	3.361(2)	
N(3)···O(1)	[2 − *X*, 0.5 + *Y*, 0.5 − *Z*]	0.01	0.2	3.430(2)	
N(3)···O(2)	[2 − *X*, 0.5 + *Y*, 0.5 − Z]	0.02	0.3	3.246(1)	
N(3)···O(9)	[1 − *X*, −0.5 + *Y*, 0.5 − *Z*]	0.04	1.0	2.779(2)	
N(5)···O(5)	[*X* − 1, *Y*, *Z*]	0.01	0.2	3.351(2)	
N(11)···O(5)	[1.5 − X, 1 − *Y*, *Z* − 0.5]	0.04	0.7	2.895(1)	
N(11)···O(8)	[*X* − 1, *Y*, *Z*]	0.02	0.3	3.275(2)	
N(13)···O(1)	[*X* − 1, *Y*, *Z*]	0.03	0.6	2.968(2)	
N(13)···O(2)	[*X* − 0.5, 0.5 − *Y*, −*Z*]	0.02	0.3	3.391(1)	
N−H···O					
N(7)−H(7)···O(2)	[*X*, *Y*, *Z*]	0.19	2.8	1.930(1)	120.98(4)
N(7)−H(7)···O(3)	[1 − *X*, Y − 0.5, 0.5 − Z]	0.03	0.5	2.799(1)	116.39(5)
N(7)−H(7)···O(11)	[0.5 + *X*, 0.5 − Y, −*Z*]	0.03	0.5	2.725(2)	111.86(3)
N(7)−H(7)···O(12)	[*X*, *Y*, *Z*]	0.16	2.9	1.896(1)	123.62(4)
C−H···O					
C(2)−H(2)···O(4)	[1 + *X*, *Y*, *Z*]	0.06	0.9	2.538(1)	104.22(4)
C(2)−H(2)···O(7)	[2 − *X*, *Y* − 0.5, 0.5 − *Z*]	0.02	0.9	2.428(1)	170.11(7)
C(4)−H(4)···O(1)	[2 − *X*, 0.5 + *Y*, 0.5 − *Z*]	0.03	0.5	2.949(1)	89.71(6)
C(4)−H(4)···O(10)	[0.5 − *X*, 1 − *Y*, 0.5 + *Z*]	0.04	0.7	2.584(1)	110.78(4)
C(4)−H(4)···O(12)	[1 − *X*, 0.5 + *Y*, 0.5 − *Z*]	0.04	1.0	2.304(1)	159.98(3)
C(10)−H(10)···O(9)	[0.5 + *X*, 1.5 − *Y*, −*Z*]	0.04	0.7	2.619(1)	93.18(4)
C(12)−H(1)···O(12)	[*X* − 0.5, 0.5 − *Y*, −*Z*]	0.04	1.1	2.298(1)	167.28(4)

[a] For some N···O contacts, critical points were not located.

and high-resolution X-ray diffraction. By deriving an experimental electron density distribution based on aspherical atomic scattering factors, and analyzing its gradient and Laplacian, one can get a far deeper insight into properties of solids than in the case of simple structural analysis.[16−18]

As the object of our study we have selected a simple model compound *N*,*N*-dipicrylamine (hereafter abbreviated as DPA; Figure 2), which is well-known to be one of the strongest organic acids.

The crystal structure of DPA exhibits a number of short intermolecular N···O contacts and potentially illustrates some trends in their electronic and structural parameters. On the basis of an experimental electron density distribution we can, in principle, characterize the N···O interactions, and N−H···O and C−H···O hydrogen bonds, in DPA in terms of critical point properties. Although the presence of critical points is commonly thought to be a necessary but not sufficient condition for the presence of weak interaction, such a characterization would allow a better understanding of the role of different types of weak interactions in molecular crystals.

Experimental Section

Crystals of the title compound (Figure 2) are yellow prisms, grown by slow evaporation from acetonitrile. Single-crystal, high-resolution, low-temperature X-ray diffraction data were collected using the Siemens SMART diffractometer and low-temperature attachment. Data reduction and empirical and analytical absorption corrections were carried out with the *SAINT* and *SADABS* programs. Crystal data and other experimental details are summarized in Table 1.

Neutron Diffraction Data Collection and Refinement. Neutron measurements were made using the time-of-flight Laue diffraction technique at a temperature of 100K, the same temperature as used in the X-ray experiment. The procedure used was similar to that described in refs 17 and 19. The crystal data and a summary of the X-ray and neutron data collections and refinements are shown in Table 1.

Multipole Refinement. The program XDLSM (described in an earlier paper[16]) of the package XD[20] was used for the multipole refinement. Anisotropic temperature factors were applied to describe the thermal motion of all atoms. Scattering factors for C, H, O, and N were derived from wave functions tabulated by Clementi and Roetti.[21] The multipole expansion was truncated at the octapole level for carbon, oxygen, and nitrogen atoms, and at the dipole level for hydrogen atoms. Since all atoms are in general positions the space group symmetry places no restrictions on the allowed multipole functions. Separate κ', κ'' were employed for aromatic C, methylene C, N, O, and H. Their values were allowed to vary, except those relating to H which were fixed at 1.2. Coordinates and anisotropic displacement parameters for the hydrogen atoms only were fixed at the values obtained from a neutron diffraction experiment (see above). We found no systematic difference between the displacement parameters for the non-hydrogen atoms obtained by X-ray and neutron diffraction. It was therefore not necessary to apply any correction to the parameters of the hydrogen atoms.[22]

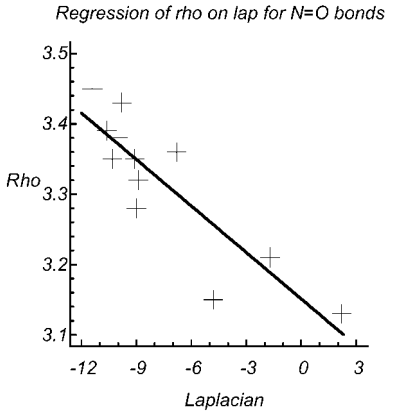

Figure 3. Linear dependence between rho [eÅ^{-3}] and Laplacian [eÅ^{-5}]: Rho = 0.022(4)Laplacian + 3.15(3), with correlation coefficient R = −0.87 for 12 N═O bonds.

Results and Discussion

Details of the final *R*-factors and goodness of fit for the 16671 reflections used in the refinement are given in Table 1. Atom

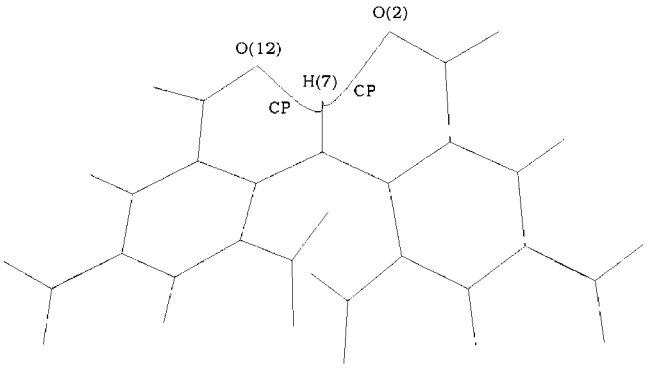

Figure 4. Interaction lines, lines along which charge is concentrated and on which critical points are situated, for bifurcated N(7)−H(7)···O(2)/O(12) hydrogen bonds. Positions of critical points are labeled CP.

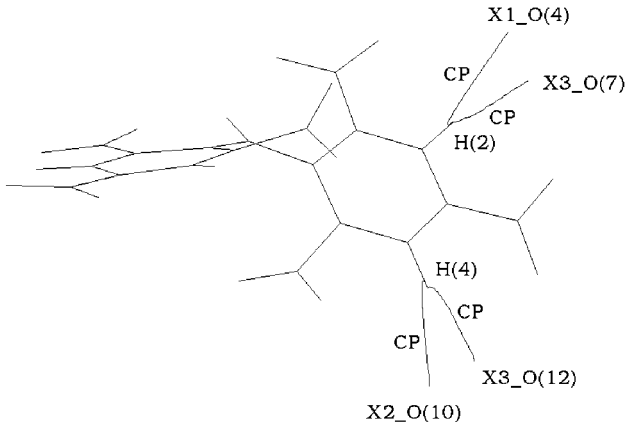

Figure 5. Interaction lines for selected bifurcated intermolecular C−H···O H-bonds to H(2) and H(4) atoms. Symmetry codes for oxygens: X1 = [1 + *X*, *Y*, *Z*], X2 = [0.5 − *X*, 1 − *Y*, 0.5 + *Z*], X3 = [2 − *X*, *Y* − 0.5, 0.5 − *Z*].

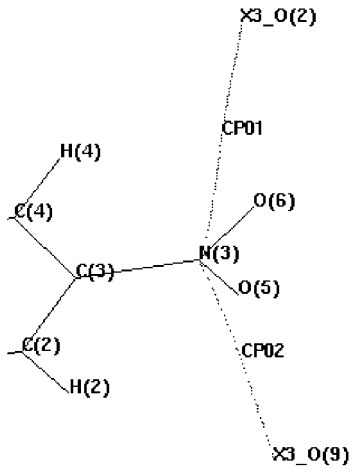

Figure 6. An example of interaction lines between the nitrogen and oxygen atoms, in the directions approximately at right angles to the plane of the nitro group.

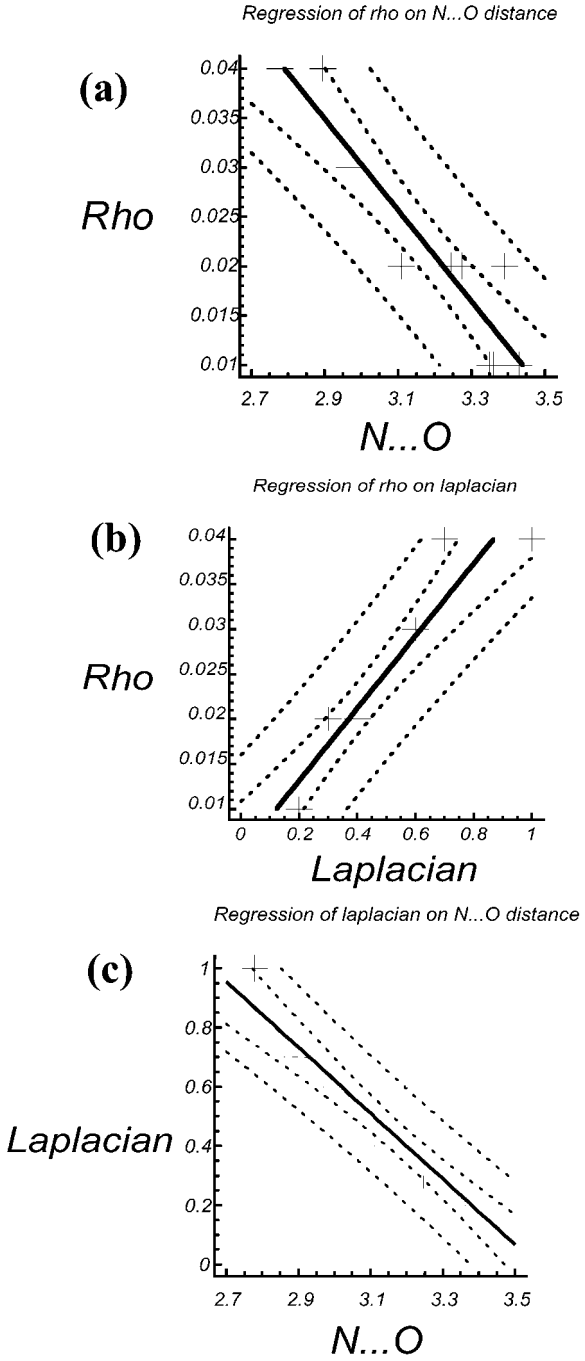

Figure 7. Linear dependence between CP parameters and N···O distances: (a) rho [eÅ^{-3}] vs N···O distance [Å], Rho = 0.17(2)[N···O] − 0.046(6), correlation coefficient $R = -0.93$, (b) rho [eÅ^{-3}] vs Laplacian [eÅ^{-5}], Rho = 0.040(5)Laplacian + 0.005(2), correlation coefficient $R = 0.94$, and (c) Laplacian [eÅ^{-5}] vs N···O distance [Å], Laplacian = −1.1(1)[N···O] + 3.9(4), correlation coefficient $R = -0.96$ for 10 N···O bonds. The dotted lines are the confidence and tolerance intervals at the significance level $\alpha = 5\%$.

labeling is shown in Figure 2. The largest residual density in the asymmetric unit appears in the region of the N(1)O(1) bond. The range of residual density values over the whole asymmetric unit is −0.276 to +0.284 eÅ^{-3}.

Four bonds fail Hirshfeld's rigid bond test,[23] with $\Delta_{A,B}$ values O(1)N(1) 0.0015, O(5)N(3) 0.0022, O(8)N(9) 0.0015, and O(9)N(11) 0.0010 Å^2. Modifications of the model by, for example, including hexadecapole terms into the multipole expansion did not lead to any decrease in the $\Delta_{A,B}$ values.

Oxygen atoms have significant negative charges as computed from the monopole populations, ranging from −0.15(5) to −0.32(4) *e*. The charges at the nitrogens are close to zero within the level of errors, with the exception of the amino nitrogen N(7) which carries charge −0.4(1) *e*. The attached hydrogen atom H(7) carries the largest positive charge equal to 0.43(5) *e*. The other hydrogens are positively charged in the range from

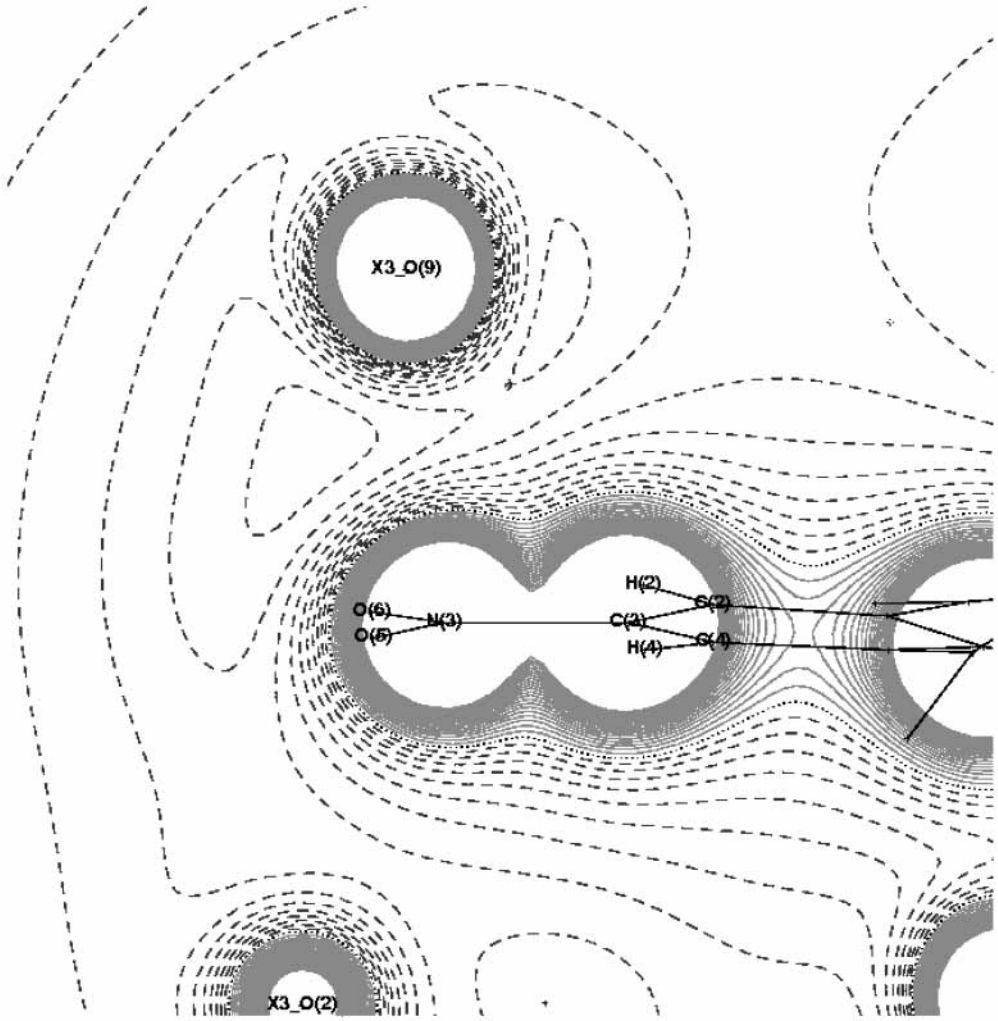

Figure 8. Electrostatic potential in the region between the nitro nitrogen and the closest oxygen atoms in a neighboring molecule. Contour interval 0.05eÅ^{-1}. Negative contours are broken. 1 eÅ^{-1} = 1388.9 kJ mol^{-1}.

0.14(3) to 0.22(3) *e*. The carbon atom charges are either close to zero or slightly positive (see Supporting Information).

The covalent bonds have typical values of critical point properties ρ_b and $\nabla^2\rho_b$. The NO bonds of the nitro groups have the highest ρ_b values [3.13(14)−3.45(7) eÅ^{-3}], consistent with their double bond character. The Laplacian values at critical points of these bonds are in the range 2.2 to −11.4 eÅ^{-5}. This variation of Laplacian values is correlated with the corresponding variation of ρ_b (see Figure 3). In our opinion the positive Laplacian value for N(1)O(1) is an indication of the uncertainty of measurements of the Laplacian values.

The bonds to the amino nitrogen N(7) have higher values of ρ_b [2.20(5) and 2.18(5) eÅ^{-3} for C(8)N(7) and C(6)N(7), respectively] than the other C−N bonds [1.67(4) to 1.85(4) eÅ^{-3}]. This is due to apparent conjugation between the nitrogen lone electron pair and the π-electron density of both aromatic rings. For example bonds to amino nitrogens in 1,8-bis-(dimethylamino)-naphthalene, DMAN,[17] have ρ_b values for CN bonds ranging from 1.7 to 2.2 eÅ^{-3}.

For the CC bonds of the aromatic rings, ρ_b ranges from 2.03-(4) to 2.27(4) eÅ^{-3}, which well compares with the values for naphthalene rings in DMAN[17] (from 1.97 to 2.37 eÅ^{-3}). For the C−H bonds the range is 1.77(6) to 1.92(6) eÅ^{-3} cf 1.83−1.95 eÅ^{-3} for DMAN.

Weak interactions in the DPA structure are of two kinds: those between nitro nitrogen atoms and oxygens in neighboring molecules (N···O), and two types of H-bonds. A relatively strong, bifurcated N−H···O H-bond and a number of weaker C−H···O bonds can be identified. The properties of all these interactions are summarized in Table 2. In general the ρ values at the CPs for weak interactions are at the level of uncertainty of measurements, which is commonly the case for such weak interactions. Some of the interactions listed in Table 2 are longer than the van der Waals distance as defined by Bondi.[24,25] We are nevertheless considering them because, in principle, such weak interactions do not vanish at the sum of the van der Waals radii. Nyburg and Faerman[26] have analyzed interatomic distances found experimentally for various elements in molecular crystals and found ranges of distances characteristic for the particular elements. They defined (not necessarily spherical) van der Waals radii in terms of the smallest interatomic distances which occur.

Some close contacts exist between amino and aromatic H-atoms and neighboring oxygen atoms. Figure 4 shows curved interaction lines for bifurcated N(7)−H(7)···O(2)/O(12) hydrogen bonds. The N−H···O interaction lines are curved close to the hydrogen, appearing to approach the critical point in the N(7)H(7) bond. This is reminiscent of the "conflict" structure generated in the dissociation of methanal into molecular H_2 and CO,[27] where a bond path links a nucleus and a bond critical point.

There are several bifurcated intermolecular C−H···O H-bonds (Table 2). Two of them, to H(2) and H(4) atoms, are illustrated in Figure 5. They show features similar to those of the NH···O interaction lines.

In the case of the N···O interactions we can identify slightly curved interaction lines between the nitrogen and oxygen atoms, in the directions approximately at right angles to the plane of the nitro group thus forming a bipyramid as shown in Figures 1 and 6. The other N···O interactions listed in Table 2 form similar pyramids or bipyramids. (3,−1) critical points in ρ exist in regions of positive Laplacian between the nitro nitrogens and the closest oxygen atoms in neighboring molecules (Table 2). These features can be interpreted by the atoms-in-molecules theory as characteristic of an attractive interaction.[28] There is also a number of weak relations between CP properties and N···O intermolecular distance (see Figure 7), such as (a) rho vs N···O, (b) rho vs Laplacian, and (c) Laplacian vs N···O internuclear distance.

An alternative representation of the density distribution in this region is shown in the form of an electrostatic potential map in Figure 8. There exists a deep potential well in the path of the N(3)···O(9) [$1 - X$, $-0.5 + Y$, $0.5 - Z$] interaction line. The potential at the (3,−1) critical point in ρ is -0.54 eÅ^{-1}, which is quite comparable with several values discussed in ref 29. Similar potentials are found for the other closest N···O contacts.

Conclusions

The DPA structure is consolidated by a number of bifurcated N−H···O and C−H···O H-bonds. Their interaction lines appear to be modified in the vicinity of the CPs of the covalent bonds of the hydrogens.

Concerning the N···O interactions, the present experimental determination of charge density in the DPA structure allows identification of interaction lines and critical points for the strongest N···O interactions including those outside Bondi's van der Waals distance. This is consistent with an attractive N···O interaction. For these weak interactions, this experiment provides a weak quantitative relationship between the charge density properties and the N−O distance.

Acknowledgment. Beam time allocation by ISIS (Chilton, U.K.) under RB7547 SXD is gratefully acknowledged.

Supporting Information Available: Fractional atomic coordinates and anisotropic displacement parameters, monopole charges, κ' and κ'' values obtained from the refinement, critical point data, multipole population coefficients, definitions of local axes, bond lengths and angles, observed and calculated structure factors, neutron fractional coordinates, neutron bond lengths and angles, neutron anisotropic temperature factors. This material is available free of charge via the Internet at http://pubs.acs.org.

References and Notes

(1) Hibbert, F.; Emsley, J. *Adv. Phys. Org. Chem.* **1990**, *26*, 255−379.
(2) Desiraju, G. R. *Angew. Chem.* **1995**, *34*, 2311−2327.
(3) Steiner, T. *Cryst. Rev.* **1996**, *6*, 1−57.
(4) Steiner, T. *Chem. Commun.* **1997**, 727.
(5) Allen, F. H.; Davies, J. E.; Galloy, J. J.; Kennard, O.; Macrae, C. F.; Mitchell, E. M.; Mitchell, G. F.; Smith, J. M.; Watson, D. G. *J. Chem. Inf. Comput. Sci.* **1991**, *31*, 187.
(6) Koch, U.; Popelier, P. L. *J. Phys. Chem.* **1995**, *99*, 9747.
(7) Bader, R. F. W. Atoms in Molecules: A Quantum Theory; Oxford University Press: Oxford, U.K. 1990.
(8) Espinosa, E.; Lacomte, C.; Molins, E. *Chem. Phys. Lett.* **1999**, *300*, 745−748.
(9) Wang, Y.; Balbuena, P. B. *J. Phys. Chem.* **2001**, *105*, 9972−9982.
(10) Desiraju, G. R.; Steiner, T. *The Weak Hydrogen Bond in Structural Chemistry and Biology*; Oxford University Press: New York, 1999.
(11) Jeffrey, G. A.; Saenger, W. *Hydrogen Bonding in Biological Structures*; Springer-Verlag: Berlin, 1991.
(12) Gavezzotti, A. *J. Phys. Chem.* **1990**, *94*, 4319.
(13) Woźniak, K.; He, H.; Klinowski, J.; Jones, W.; Grech. E. *J. Phys. Chem.* **1994**, *98*, 13755−13765.
(14) Howard, S. T.; Platts, J. A.; Woźniak, K. *Chem. Phys. Lett.* **1995**, *232*, 479−485.
(15) Woźniak, K. *Pol. J. Chem.* **1997**, *71*, 6, 779-791.
(16) Mallinson, P. R.; Woźniak, K.; Smith G. T.; McCormack, K. L. *J. Am. Chem. Soc.* **1997**, *119*, 11502−11509.
(17) Mallinson, P. R.; Woźniak, K.; Wilson, C. C.; McCormack, K. L.; Yufit, D. S. *J. Am. Chem. Soc.* **1999**, *121*, 4640−4646.
(18) Koritsanszky, T. S.; Coppens, P. *Chem. Rev.* **2001**, *101*, 1583−1627.
(19) Woźniak, K.; Wilson, C. C.; Knight, K. S.; Grech, E. *Acta Crystallogr.* **1996**, *B52*, 691−696.
(20) Koritsanszky, T. S.; Howard, S.; Richter, T.; Mallinson, P. R.; Su, Z.; Hansen, N. K. XD, a computer program package for multipole refinement and analysis of charge densities from X-ray diffraction data. Free University of Berlin, Germany; University of Wales, Cardiff, UK.; University of Glasgow, UK.; University of Buffalo, Buffalo, New York; University of Nancy, France, 1995.
(21) Clementi, E.; Roetti, C. *At. Data Nucl. Data Tables* **1974**, *14*, 177−478.
(22) Blessing, R. H. *Acta Crystallogr.* **1995**, *A51*, 33−38.
(23) Hirshfeld, F. L. *Acta Crystallogr.* **1976**, *A32*, 239−244.
(24) Bondi, A. J. *Phys. Chem.* **1964**, *68*, 441−451.
(25) Bondi, A. *Physical Properties of Molecular Crystals, Liquids and Glasses*; John Wiley: New York, 1984; pp 450ff.
(26) Nyburg, S. C.; Faerman, C. H. *Acta Crystallogr.* **1985**, *B41*, 274−279.
(27) Popelier, P. *Atoms-In−Molecules−An Introduction*; Prentice Hall: New York, 2000; Chapter 6, pp 81−95.
(28) Bader, R. F. W. *J. Phys. Chem. A* **1998**, *102*, 7314−7323.
(29) Coppens, P. *X-ray Charge Densities and Chemical Bonding*; International Union of Crystallography and Oxford University Press: New York, 1997; pp 165−192.